

Enhancement of CO₂ Adsorption Containing Zinc-ion-exchanged Zeolite NaA Synthesized from Rice Husk Ash

Patchaya Tobameekul, Supawon Sangsuradet and Nareerat Na Chat

Department of Chemical Engineering, Faculty of Engineering, King Mongkut's University of Technology North Bangkok, Bangkok, Thailand

Patcharin Worathanakul*

Department of Chemical Engineering, Faculty of Engineering, King Mongkut's University of Technology North Bangkok, Bangkok, Thailand

Center of Eco-Materials and Cleaner Technology (CECT), Science and Technology Research Institute, King Mongkut's University of Technology North Bangkok, Bangkok, Thailand

* Corresponding author. E-mail: patcharin.w@eng.kmutnb.ac.th DOI: 10.14416/j.asep.2020.11.006

Received: 8 June 2020; Revised: 18 August 2020; Accepted: 16 September 2020; Published online: 12 November 2020

© 2022 King Mongkut's University of Technology North Bangkok. All Rights Reserved.

Abstract

Carbon dioxide is the main cause of the greenhouse effect and it contributes to global warming. Zeolite NaA is an excellent adsorbent among other materials but its potential as a carbon dioxide adsorption still needs to be developed. Therefore, this research was to synthesize zeolite NaA from rice husk ash under different temperatures and crystallization times. The synthesized zeolite NaA was modified with zinc by an ion exchange method. Adsorbents were tested for the carbon dioxide adsorption at different operating temperatures and flow rates. The results showed that the zeolite NaA was successfully synthesized from rice husk ash under the optimal condition of the crystallization temperature at 333.15 K and time for 2 h. The zeolite NaA can be synthesized at low temperature and time for crystallization resulted in low cost absorbent while achieving high efficiency. The modification of zeolite NaA with zinc played a key role to increase the BET surface area, micropore volume and total pore volume and resulted in an increase in carbon dioxide adsorption capacity. High carbon dioxide adsorption at 89.08% with the operating temperature at 573.15 K and carbon dioxide flow rate of 1 L/h were shown with 5 wt.% zeolite NaA.

Keywords: Zeolite NaA, Rice husk ash, Zinc, Ion exchange method, Carbon dioxide adsorption

1 Introduction

Climate change is one of the most urgent environmental problems caused by greenhouse gas emission from human activities [1]. Carbon dioxide (CO₂) is considered as a major greenhouse gas for accelerating global warming. The main CO₂ sources could be released from cement industries and power plants etc. [2]. In 2019, CO₂ emissions from natural gas, coal and oil in electricity

generation are 94.2 million tonnes of CO₂. The CO₂ emissions have decreased by 5% compared to 2018. Renewable sources are used instead of coal as a fuel to generate electricity. Currently, renewable sources, such as biomass power plant are used to generate electricity about 10% of the total electricity generation [3], but they also produce various pollutants, such as nitrogen oxides (NO_x), sulphur oxides (SO_x), carbon monoxide (CO), water, particulates and CO₂ [4].

Consequently, the CO₂ capture from the use operation biomass power plants in electricity generation needs to be developed to reduce CO₂ emissions. The CO₂ capture and storage (CCS) technology is considered. Post-combustion CO₂ capture technology has become one of the important options to reduce CO₂ emissions, as important green and economic technology [5]. The solvent absorption, cryogenics, membranes and solid adsorption methods can be employed in this technology [6]. The solvent absorption, cryogenics and membranes have disadvantages such as corrosion problems, requires high cost, high energy consumption and regeneration. Solid adsorption as the adsorbents could provide superior advantages over conventional methods. It requires lower energy consumption, simpler processes and lower environmental effects [7]. Typical adsorbents are zeolites, activated carbons and metal-organic frameworks, etc. [8].

Zeolite is one of the most promising adsorbents for CO₂ capture application. It is a high surface area, strong dipole–quadrupole, inexpensive, thermal and mechanical stability [7], [9]. In previous researches, synthesis and characterization of zeolites for CO₂ adsorption such as NaA, NaX, NaY, ZSM-5 and T-type zeolite were investigated [1], [9]–[12]. The appropriate choice of zeolites for CO₂ adsorption depends on numerous factors such as Si/Al ratio, polarity properties and the number of cations, etc. [2], [7], [13]. Salehi *et al.* [13] reported that the zeolite NaX and NaA exhibit higher CO₂ adsorption capacity than zeolite NaY at atmospheric pressure and 298 K. Due to zeolite NaX and NaA have a lower Si/Al ratio than zeolite NaY, the presence of the larger surface area, more alkali-ions in the zeolite frameworks and the stronger dipole–quadrupole exhibit stronger CO₂ adsorption capacity. The Si/Al ratio of zeolite NaX and NaA are approximately 1. While zeolite NaY has the same structural framework as zeolite NaX, but it has a Si/Al ratio of approximately 3 and lower cations. Likewise, Yi *et al.* [14] also studied adsorption on zeolites FAU and LTA. The zeolite NaY has a lower CO₂ adsorption capacity than zeolite CaA and NaX. Because zeolite NaY has a higher Si/Al ratio than zeolite CaA and NaX, zeolite NaY exhibits more non-polar and weaker interactions between CO₂ and cations. On the other hand, zeolite CaA has more negative charge, which makes its high polar. While zeolite NaX and NaY have the same structure, but zeolite NaX presents higher polar due to its lower Si/Al ratio.

Among them, Zeolite A has exquisite properties showing high selectivity toward CO₂ adsorption and regenerability [10], due to its diameter size of 4 Å that is highly versatile molecular sieve including the three-dimensional pore structure and solid acidity [15]. But, its potential as a CO₂ capture adsorbent still needs to be developed. Therefore, the behavior of zeolite A under different synthesis conditions and modification of structure including the adsorption process needs to be investigated. Zeolite A can be prepared with alumina-rich and silica-rich materials [15]. Rice husk ash (RHA) is silica-rich material obtained from biomass power plant, which is suitable to produce a low cost zeolite for CO₂ capture [16]. The silica extraction from RHA in zeolite synthesis is one of the solutions to add value to RHA and reduce the amount of RHA waste [12]. Normally, silica extraction has many methods, such as pyrolysis and solvent extraction methods. The solvent extraction method was chosen to produce silica because it is produced at lower temperatures, lower amounts of energy, lower cost and larger amounts of silica [17].

In general, zeolite NaA is prepared by hydrothermal method from silicate and aluminate solution. There are many synthesis techniques of conventional hydrothermal methods, such as autoclave or in oven operations [13], [18], [19]. In addition, many authors have reported for zeolite NaA synthesis using other sources, such as ultrasound and microwave heating. It is a new method and very simple, but this technique also takes a high temperature and a long time to crystallize the zeolite NaA [20], [21]. There are many researchers who have investigated effects of crystallization temperatures and time [18]–[22]. Among the conventional methods, all techniques also take a high temperature and a long time of crystallization. Therefore, crystallization at low temperature and short time is still being developed to obtain zeolite NaA with a high degree of purity as well as to reduce the cost of synthesis.

The CO₂ adsorption from large volume at high temperature of flue gases is still expensive and high energy consumption [7], [8]. In order to modify zeolite for CO₂ adsorption at high temperature, decrease the cost and increase the efficiency of zeolites for CO₂ adsorption need to be developed. Surface modification of the zeolite could enhance the CO₂ adsorption capacity by increasing the alkalinity and cation incorporated to the zeolite structure [8], [23]. Several authors have shown that surface and chemical properties of zeolite

can be improved by incipient wetness impregnation and aqueous solution ion exchanged methods [2], [24], [25]. The results showed that Ni (II) was successfully incorporated into zeolite Y with the impregnation and ion exchange method. The Ni (II) loading in both methods does not affect the zeolite Y structure. Worathanakul and Saisuwansiri [26] reported that Cu and Fe impregnated zeolite Y show higher adsorption capacities than the pure zeolite Y. In another study, Chen *et al.* [27] reported that Li^+ , Pd^{2+} , and Ag^+ exchanged zeolite 13X show better CO_2 adsorption capacity than the pure zeolite 13X. Zeolite LiPdAgX showed the highest CO_2 adsorption capacity due to its high number of adsorption sites and thermal conductivities. Among these methods, the aqueous solution ion exchanged method is one of the most commonly used methods. The degree of ion exchange depends on the size and charge of the metal ion [28].

Smykowski *et al.* [29] have studied CO_2 adsorption on Cu, Zn, Ni, Pd/DOH zeolite by DFT method. Zinc cation has a stronger interaction with the CO_2 molecule than other cations, which leads to stronger CO_2 adsorption. In addition, Esquivel *et al.* [30] have found that Zn (II) exchanged zeolite beta is generated Lewis acid sites and redox properties to modify the surface charge characteristics of zeolite. According to reports on adsorbent modification, there is no report of Zn-ion-exchanged zeolite NaA for CO_2 adsorption. Therefore, the developmental of a novel zeolite can offer desired properties of cost and adsorption capacity with the most important challenges.

The objective of this research was to develop zeolite NaA synthesized from RHA at Si/Al ratio of 1. The effects of crystallization temperature and time on the zeolite NaA synthesis were investigated in this work. The zeolite NaA was modified with different weight percentages (wt.%) of zinc by an ion exchange method to improve CO_2 adsorption capacity from biomass power plant flue gas. The CO_2 adsorption on the adsorbent was examined at different operating temperatures and CO_2 flow rates.

2 Materials and Methods

2.1 Materials

Silica and zeolite NaA adsorbents were prepared by

reacting the following: RHA obtained from U-Thong biomass Co, LTD., Thailand (contains 70.19 wt.% SiO_2), hydrochloric acid (HCl, Merck, Germany), sodium aluminate (NaAlO_2 , Sigma Aldrich, Singapore), sodium hydroxide (NaOH, Merck, Germany), zinc nitrate ($\text{Zn}(\text{NO}_3)_2 \cdot 6\text{H}_2\text{O}$, Merck, Germany), distilled water and deionized water (DI).

2.2 Silica extraction

The methodology used to pretreat RHA before silica extraction is based on the works of An *et al.* [31] with modifications in the boiling time to remove the metallic ions completely. 5 g of RHA was mixed with 1 M HCL solution and boiled for 1 h under stirring. The suspension solutions were separated through filtration and washed with DI water. The solid residue was dried at 393.15 K for 12 h. The RHA after pretreatment was mixed with 2 M NaOH solution at 343.15 K for 1 h. The solutions were separated through filtration and mixed with 1 M HCL solution until the pH became 7. Then, the solution was aged at room temperature for 18 h. The gel product was separated through filtration and washed with distilled water to obtain solid of silica. The product was dried at 378.15 K for 12 h. The silica in the form of Na_2SiO_3 was obtained.

2.3 Zeolite NaA synthesis

According to the research of Cheung *et al.* [32] and Worathanakul *et al.* [33], have found that the better crystallinity was obtained for zeolite NaA at crystallized temperatures higher than 313.15 K and 2 h. While, crystallization at lower temperatures and shorter times showed a low degree of crystallinity resulting in poorly crystallized samples. In order to get a synthesis with lower energy consumption and higher efficiency, the heat crystallization at 333.15 and 373.15 K for 2 and 4 h were selected in this study. Zeolite NaA synthesis was carried out following the experimental procedure reported by Worathanakul *et al.* [33] with different crystallization temperatures and times. Initially, the NaOH was mixed with DI water, divided into two equal volumes (B1 and B2). The NaAlO_2 was added into B1 solution and stirred for 10 min (V1). The Na_2SiO_3 from RHA and NaOH was placed in B2 solution and stirred for 10 min (V2). Then, the V1 solution was slowly added to the V2 solution under stirring until

homogenous. The obtained sample was heated at different temperatures (333.15 and 373.15 K) and times (2 and 4 h) of heat crystallization. The solutions were separated through filtration and washed with DI water until the pH was below 9. The crystalline zeolite was dried at 378.15 K for 8 h. The pure zeolite NaA powder was obtained.

2.4 Modification of Zeolite NaA

The zeolite NaA was modified with different wt.% of zinc loadings (1, 3 and 5 wt.%) by ion exchanged method. The obtained zeolite NaA powders were added to the 1 wt.% Zn aqueous solution and stirred at room temperature for 24 h. The suspension solutions were separated through filtration and washed with DI water. Finally, the samples were dried at 393.15 K for 12 h and calcined at 873.15 K for 5 h. The 1 zeolite ZnA powder was obtained. In addition, the 1 wt.% of Zn aqueous solution was changed to 3 wt.% and 5 wt.% of Zn aqueous solution by repeating in the above steps to Zn loading to zeolite NaA. The modified zeolite NaA with 1, 3 and 5 wt.% Zn loadings were denoted as 1 zeolite ZnA, 3 zeolite ZnA and 5 zeolite ZnA, respectively.

2.5 Characterization analysis

The chemical composition of RHA was examined by X-ray fluorescence spectroscopy (XRF, Bruker AXS, Germany). The purity and modification of zeolite NaA were explored by X-ray diffraction analysis (XRD, Bruker AXS, Germany). In order to characterize the morphology of the obtained samples, the SEM images were identified by field emission scanning electron microscopy (FESEM, JSM-7001F, JEOL, Tokyo, Japan). The surface area and porosity of the obtained samples were determined with Brunauer–Emmett–Teller analysis (BET, Autosorb 1C, Quantachrome, USA).

2.6 CO₂ adsorption measurement

Flue gas from biomass power plants typically contains NO_x, SO_x, CO, CO₂, water and particulates. In this study, it is assumed that NO_x, SO_x, CO, H₂O and particulates are removed after the pretreatment process, so that the feed flue gas contains CO₂. In the present study, the flue gas from the power plant is released at

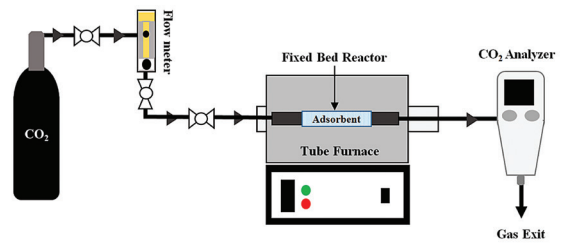


Figure 1: Experimental setup for CO₂ adsorption.

temperature in the range of 313.15 to above 573.15 K with a total pressure of approximately 1 atm, depending on the design and operation of the process [6], [34]. Therefore, this research is conducted at a temperature of 373.15, 573.15 and 873.15 K.

The experimental work was set up with a gas flow meter, adsorption column, tube furnace for heating and CO₂ analyzer (Handheld CO₂ meter GM 70, Finland) shown in Figure 1. The samples were prepared in a packed bed reactor and placed inside the tube furnace. Then, the adsorption experiments were carried out at different temperatures (373.15, 573.15 and 873.15 K) and flow rates (1, 3 and 5 L/h) of pure CO₂ (99.80%: HP Grade, Linde, Thailand). All samples were performed at atmospheric pressure and the adsorption time for 2 h. The inlet (C_0) and outlet (C) concentration of CO₂ were monitored to obtain the data required for calculation of CO₂ conversion and breakthrough curve according to Equations (1) and (2), respectively.

$$\%CO_2 \text{ Conversion} = \frac{C_0 - C}{C_0} \times 100 \quad (1)$$

$$\text{Breakthrough curve} = \frac{C}{C_0} \quad (2)$$

3 Results and Discussion

3.1 Silica extraction

After extraction, the sample was composed of 97.73, 2.24 and 0.03% by the gross weight of silicon dioxide (SiO₂), aluminum oxide (Al₂O₃) and iron oxide (Fe₂O₃), respectively. Furthermore, XRF data showed that the after extraction of SiO₂, it contained a very small amount of impurity. The obtained SiO₂ after extraction from RHA was the highest compared to unextracted sample. These results have been

corresponded with studies by An and co-workers [31]. the most of impurity contents were removed after treatment with HCl, which resulted from the chemical reaction between acid and metals. Chloride ion (Cl^-) from HCl protonated the silicon (Si) and formed silicon chloride (SiCl_4) during the treatment with HCl. Thus, obtained SiCl_4 was insoluble resulting in silicon, which was not removed during the treatment with HCl. While treatment with HCl, the Cl^- from HCl will react to the metallic element (potassium: K, sodium: Na, zinc: Zn, magnesium: Mg, copper: Cu, calcium: Ca, manganese: Mn and iron: Fe) and formed salts (potassium chloride: KCl, sodium chloride: NaCl, zinc chloride: ZnCl_2 , magnesium chloride: MgCl_2 , copper chloride: CuCl_2 , calcium chloride: CaCl_2 , manganese chloride: MnCl_2 , iron chloride: FeCl_3). The metallic chloride obtained was soluble resulting in metallic, which was dissolved and removed by filtration. This result was corresponded with a study by Matori *et al.* [35]. The result also showed that the RHA pretreatment with the boiling time of 1 h was highly effective for removing the metallic ions compared to RHA pretreatment and was similar to the work of An *et al.* [31]. Therefore, extracted SiO_2 could be an effective way to produce high purity of SiO_2 powder.

3.2 Zeolite NaA synthesis

3.2.1 Effect of temperature and time

Figure 2(a) shows the XRD patterns of samples prepared with different temperatures (333.15 and 373.15 K) and times (2 and 4 h) of heat crystallization. The XRD results showed that zeolite NaA was the main peak corresponded to peaks standards. It can be seen that the width of peaks was decreased with increasing crystallization temperature and time resulting in increased crystal size corresponds to the research of Jin *et al.* [36]. The obtained results were also consistent with Cheung *et al.* [32] reported the crystallization temperature and time were related to the crystal quality of zeolite NaA. Moreover, the temperature and time in our zeolite NaA synthesis were still lower than the previous study and zeolite NaA still has good performance [32]. The SEM images for different temperatures (333.15 and 373.15 K) and times (2 and 4 h) of heat crystallization [Figure 2(b)–(e)] show particles with spherical structure, uniform distribution and

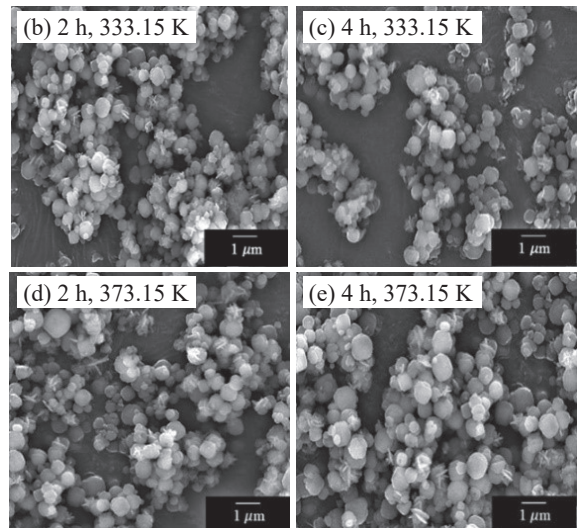
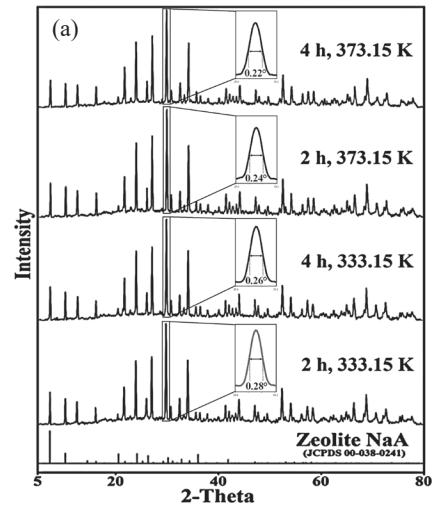


Figure 2: XRD patterns and SEM images of zeolite NaA with different temperatures and times of heat crystallization.

highly crystalline structure. Figure 2(b) to (e) indicated that crystal sizes were 0.30 ± 0.06 , 0.34 ± 0.03 , 0.39 ± 0.02 and 0.42 ± 0.03 μm diameter, respectively corresponds to the research of Worathanakul *et al.* [33]. The reduction of crystallization temperature and time in this novel synthesis method was a successfully developed process zeolite NaA synthesis with short time and low temperature. This can also help the reduction of time and energy consumption of the synthesis. Thus, the optimum heat crystallization for the zeolite NaA synthesis from RHA was 333.15 K for 2 h, where high

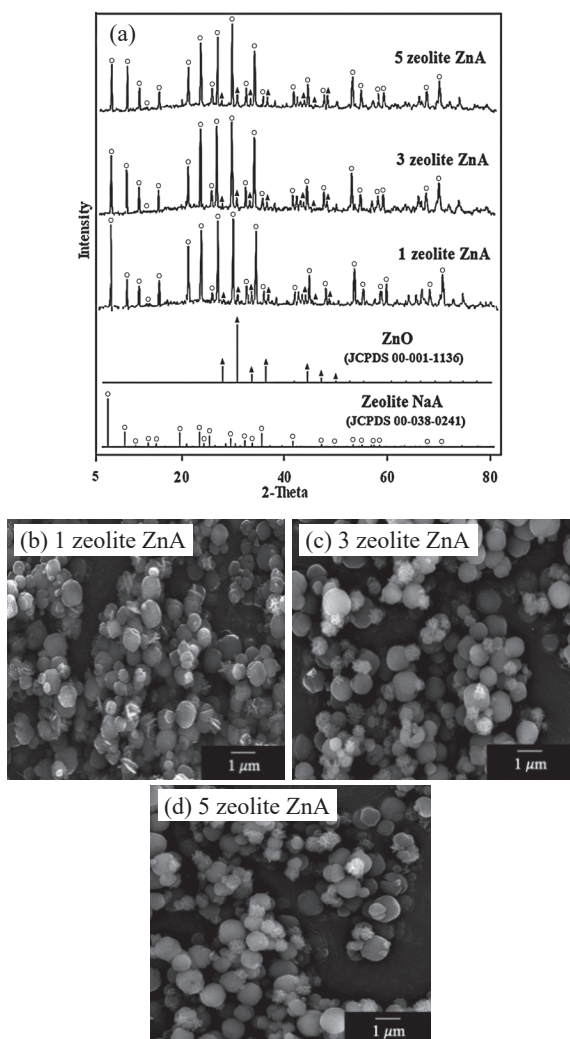


Figure 3: XRD patterns and SEM images on zeolite NaA with different wt.% of Zn loadings.

purity zeolite NaA at low crystallization temperature and time were optimized and used throughout the entire experiments.

3.2.2 Effect of Zn loading

The effect of Zn loading on the structural properties of zeolite NaA was investigated by XRD shown in Figure 3(a). The XRD patterns show that zeolite NaA after loading Zn was the main peak that corresponded to standard peaks of zeolite NaA. It can be observed that the structural integrity of zeolite NaA was maintained

the same structure even after the incorporation of the Zn [37]. Particles of 1 zeolite ZnA, 3 zeolite ZnA and 5 zeolite ZnA had uniform distribution as shown in Figure 3(b)–(d), respectively. The crystals have a similar size of approximately $0.33 \pm 0.08 \mu\text{m}$ diameter.

BET analysis of zeolite NaA with different wt.% of Zn loadings by ion exchange method was shown in Table 1. As the wt.% of Zn loading increased, the BET surface area, micropore volume and total pore volume of the zeolite were increased. The high surface area suggested that more active sites were available on the zeolite, which were useful for the enhancement of the CO_2 conversion [17]. It is apparent that the addition of Zn^{2+} to the zeolite NaA improved the BET surface areas and pore volumes. In contrast, the pore size showed a decreasing trend with an increased from 1 to 3 wt.% Zn loading, due to loaded Zn caused blockage some pores of some the zeolite NaA. Zn^{2+} can be the main one exchange with two Na and the two types of cation occupying different sites in zeolite crystal. It caused partial blockage of pores and released some pores of the zeolite simultaneously, which corresponded to the research of Chen *et al.* and Salehi and Anbia [13], [27]. Based on the above reasons, it did not affect the increase of the BET surface area of zeolite NaA, which is similar to the report of Zhang *et al.* [17]. Therefore, the 5 zeolite ZnA was used throughout the CO_2 adsorption experiments.

Table 1: BET analysis of Zn loading to zeolite NaA

Samples	BET Surface Area (m^2/g)	Micropore Volume (cm^3/g)	Total Pore Volume (cm^3/g)	Pore Diameter (\AA)
Zeolite NaA	29.58	0.015	0.103	22.27
1 zeolite ZnA	35.42	0.018	0.146	21.18
3 zeolite ZnA	54.30	0.023	0.212	19.46
5 zeolite ZnA	73.94	0.029	0.286	18.03

3.3 CO_2 adsorption capacity

3.3.1 Effect of Zn loading

The effect of Zn loading was focused in this section. The experimental data was performed with the constant operating temperature at 573.15 K and the CO_2 flow

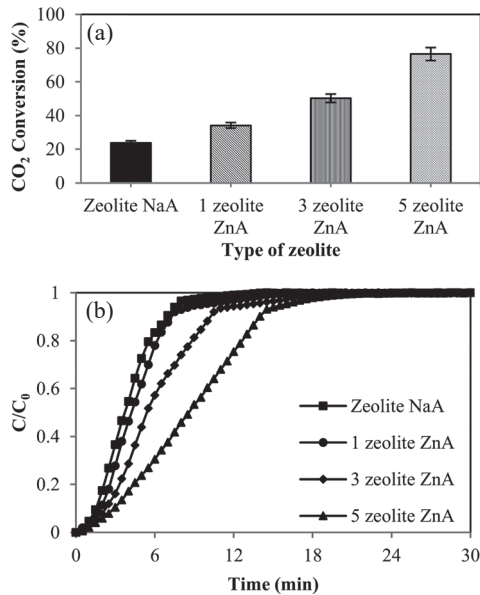


Figure 4: CO₂ conversion and breakthrough curves of zeolite NaA with different wt.% of Zn loadings for CO₂ adsorption at 573.15 K and flow rate of 5 L/h.

rate of 5 L/h. As shown in Figure 4(a), the %CO₂ conversion was increased with increasing of Zn loading to zeolite NaA. The CO₂ adsorption of the 5 zeolite ZnA was observed that it was increased by approximately 3.5 times when compared to that of the zeolite NaA. It was corresponding to the results of BET analysis. As it was apparent from Figure 4(b), the breakthrough curve of 5 zeolite ZnA did not change much. The breakthrough curve of zeolite NaA sharply increased in the behavior at first and increased slightly until gradually constant, which may attribute to the fastest diffusivity [26]. Similar behavior breakthrough curve of 1 zeolite ZnA and 3 zeolite ZnA were found. It was implied the 5 zeolite ZnA was beneficial for CO₂ adsorption under experimental conditions.

3.3.2 Effect of operating temperature

In order to study the effect of operating temperature on 5 zeolite ZnA, the experiments have been carried out under the operating temperature at 373.15, 573.15 and 873.15 K with a CO₂ flow rate of 5 L/h. The 5 zeolite ZnA showed that the %CO₂ conversion increased in the order: 573.15 K > 373.15 K > 873.15 K as can be seen in Figure 5(a). It can be seen that the operating

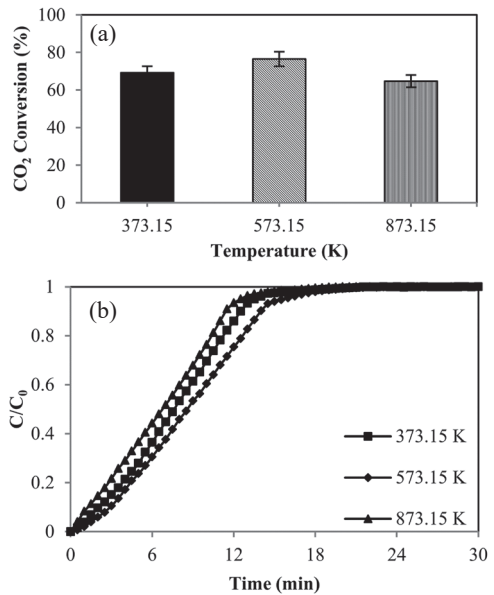


Figure 5: CO₂ conversion and breakthrough curves of 5 zeolite ZnA with different operating temperatures (373.15, 573.15 and 873.15 K) and CO₂ flow rate of 5 L/h.

temperature at 373.15 K 5 has lower adsorption than 573.15 K as a result of physical adsorption dominance over chemical adsorption. The obtained results were consistent with Ramasubramanian *et al.* [38] that the physical adsorption showed lower adsorption than chemical adsorption. Due to the physical adsorption, it is caused by the weak interaction between the zeolite and CO₂ molecules occur via van der Waals forces in the pores of zeolite and the electrostatic interaction of the zeolite surface groups [39], [40]. At 573.15 K, it showed chemical adsorption was the dominant process due to the incorporation of the Zn in the zeolite NaA. There is an increase in the adsorption at 573.15 K that was observed due to an increase in the chemical adsorption process. Chemical adsorption arises from relatively strong chemical interactions between the Zn and CO₂ molecules with chemical bonds [6], [38]. In contrast, the adsorbent was desorbed of CO₂ at 873.15 K. These results agreed with reports of Pirngruber *et al.* [41] that the decrease of the adsorption was caused by the exothermicity of the adsorbent. The breakthrough curves demonstrated that the shape at the first phase of 573.15 K was not changed much. Figure 5(b) represented the breakthrough curve at 373.15 and 873.15 K show sharply increased first and constant curve, which

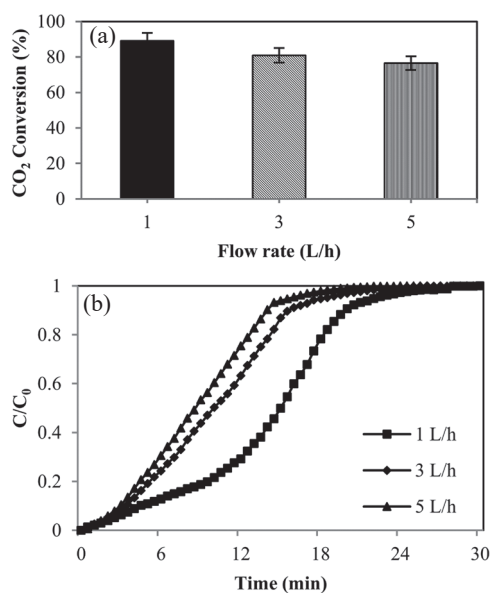


Figure 6: CO₂ conversion and breakthrough curves of 5 zeolite ZnA with different CO₂ flow rates (1, 3 and 5 L/h) and operating temperature at 573.15 K.

may attribute to the fastest diffusivity. Both curves were presented a trend to saturation of CO₂ adsorption. While, the adsorbents at 573.15 K were found that CO₂ was still diffused in the upstream, and began to breakthrough and gradually constant curve. The results showed that operating temperature at 573.15 K could have high CO₂ adsorption with 5 zeolite ZnA.

3.3.3 Effect of CO₂ flow rate

To find out the effect of CO₂ flow rate on 5 zeolite ZnA, the CO₂ adsorption studies were conducted with different flow rates (1, 3 and 5 L/h) and fixed the operating temperature at 573.15 K. Figure 6(a) showed that the %CO₂ conversion rapidly decreased with an increasing flow rate of CO₂ from 1 to 5 L/h. The CO₂ adsorption at 1 L/h of rate flow was more than 3 times with at 5 L/h, due to the total adsorption operating time drastically decreased with increasing of the CO₂ flow rate [42]. The shape of CO₂ flow rate at 1 L/h breakthrough curve was not changed much as shown in Figure 6(b) because of trapped CO₂ in the adsorbents. With increasing the CO₂ flow rate (3 and 5 L/h), the breakthrough curves became sudden at first. It may be the fastest diffusivity. After that, the CO₂ concentration adsorbed

to breakthrough increased slightly and constant. Both curves were fit to the trend to saturation. The results showed that the CO₂ flow rate at 1 L/h with 5 zeolite ZnA could have high CO₂ adsorption, due to the residence time of CO₂ molecules at a low flow rate was longer than with high flow rates [33].

4 Conclusions

The optimal condition for the zeolite NaA synthesis from RHA was 2 h at 333.15 K with high purity zeolite NaA at low crystallization temperature and time. The obtained zeolite NaA particles exhibit spherical morphology with uniform size distribution. After ion exchange, the BET surface area, micropore volume and total pore volume of 5 zeolite ZnA were higher than 1 zeolite ZnA with the same structure. The highest CO₂ adsorption was found in the operating temperature at 573.15 K and CO₂ flow rate of 1 L/h. Zn plays a key role to improve the CO₂ adsorption capacity on zeolite NaA. In addition, this adsorbent is lower energy consumption and low synthesis cost with high efficiency. These properties make it promising candidate adsorbents for further application of CO₂ adsorption in hot flue gas from biomass power plants.

Acknowledgments

This research was financially supported by the Thailand Research Fund (TRF), contract no. PHD5910018 and U-Thong biomass Company Limited. We also acknowledge Graduate school of King Mongkut's University of Technology North Bangkok.

References

- [1] Y. Wang, T. Du, Z. Qiu, Y. Song, S. Che, and X. Fang, "CO₂ adsorption on polyethylenimine-modified ZSM-5 zeolite synthesized from rice husk ash," *Materials Chemistry and Physics*, vol. 207, pp. 105–113, 2018.
- [2] M. Vinoba, M. Bhagiyalakshmi, Y. Alqaheem, A. A. Alomair, A. Pérez, and M. S. Rana, "Recent progress of fillers in mixed matrix membranes for CO₂ separation: A review," *Separation and Purification Technology*, vol. 188, pp. 431–450, 2017.
- [3] Energy Policy and Planning office (EPPO),

- “Carbon dioxide (CO₂) emissions from energy consumption in 2019,” Energy Policy and Planning office (EPPO), Ministry of Energy, Bangkok, Thailand.
- [4] H. Liu, G. Qiu, Y. Shao, and S. B. Riffat, “Experimental investigation on flue gas emissions of a domestic biomass boiler under normal and idle combustion conditions,” *International Journal of Low-Carbon Technologies*, vol. 5, pp. 88–95, 2010.
- [5] B. Acar, M. S. Başar, B. M. Eropak, B. S. Caglayan, and A. E. Aksoylu, “CO₂ adsorption over modified AC samples: A new methodology for determining selectivity,” *Catalysis Today*, vol. 301, pp. 112–124, 2018.
- [6] P. Ammendola, F. Raganati, and R. Chirone, “CO₂ adsorption on a fine activated carbon in a sound assisted fluidized bed: Thermodynamics and kinetics,” *Chemical Engineering Journal*, vol. 322, pp. 302–313, 2017.
- [7] S. Y. Lee and S. J. Park, “A review on solid adsorbents for carbon dioxide capture,” *Journal of Industrial and Engineering Chemistry*, vol. 23, pp. 1–11, 2015.
- [8] M. Younas, M. Sohail, L. K. Leong, M. J. K. Bashir, and S. Sumathi, “Feasibility of CO₂ adsorption by solid adsorbents: A review on low-temperature systems,” *International Journal of Environmental Science and Technology*, vol. 13, pp. 1839–1860, 2016.
- [9] Q. Jiang, J. Rentschler, G. Sethia, S. Weinman, R. Perrone, and K. Liu, “Synthesis of T-type zeolite nanoparticles for the separation of CO₂/N₂ and CO₂/CH₄ by adsorption process,” *Chemical Engineering Journal*, vol. 230, pp. 380–388, 2013.
- [10] Z. Bacsik, O. Cheung, P. Vasiliev, and N. Hedin, “Selective separation of CO₂ and CH₄ for biogas upgrading on zeolite NaKA and SAPO-56,” *Applied Energy*, vol. 162, pp. 613–621, 2016.
- [11] L. Yu, J. Gong, C. Zeng, and L. Zhang, “Synthesis of binderless zeolite X microspheres and their CO₂ adsorption properties,” *Separation and Purification Technology*, vol. 118, pp. 188–195, 2013.
- [12] R. M. Mohamed, I. A. Mkhaliid, and M. A. Barakat, “Rice husk ash as a renewable source for the production of zeolite NaY and its characterization,” *Arabian Journal of Chemistry*, vol. 8, pp. 48–53, 2015.
- [13] S. Salehi and M. Anbia, “Characterization of CPs/Ca-exchanged FAU- and LTA-type zeolite nanocomposites and their selectivity for CO₂ and N₂ adsorption,” *Journal of Physics and Chemistry of Solids*, vol. 110, pp. 116–128, 2017.
- [14] H. Yi, H. Deng, X. Tang, Q. Yu, X. Zhou, and H. Liu, “Adsorption equilibrium and kinetics for SO₂, NO, CO₂ on zeolites FAU and LTA,” *Journal of Hazardous Materials*, vol. 203–204, pp. 111–117, 2012.
- [15] A. R. Loiola, J. C. R. A. Andrade, J. M. Sasaki, and L. R. D. da Silva, “Structural analysis of zeolite NaA synthesized by a cost-effective hydrothermal method using kaolin and its use as water softener,” *Journal of Colloid and Interface Science*, vol. 367, pp. 34–39, 2012.
- [16] W. Panpa and S. Jinawath, “Synthesis of ZSM-5 zeolite and silicalite from rice husk ash,” *Applied Catalysis B: Environmental*, vol. 90, pp. 389–394, 2009.
- [17] I. J. Fernandes, D. Calheiro, F. A. L. Sánchez, A. L. D. Camacho, T. L. A. C. Rocha, C. A. Moraes, and V. C. Sousa, “Characterization of silica produced from rice husk ash: Comparison of purification and processing methods,” *Journal of Materials Research*, vol. 20, pp. 512–518, 2017.
- [18] M. Mirfendereski and T. Mohammadi, “Effects of synthesis parameters on the characteristics of Naa type zeolite nanoparticles,” in *Proceedings of the World Congress on Recent Advances in Nanotechnology (RAN’16)*, 2016, pp. ICNNFC 113.
- [19] A. A. B. Maia, R. N. Dias, R. S. Angélica, and R. F. Neves, “Influence of an aging step on the synthesis of zeolite NaA from Brazilian Amazon kaolin waste,” *Journal of Materials Research and Technology*, vol. 8, pp. 2924–2929, 2019.
- [20] S. N. Azizi and M. Yousefpour, “Synthesis of zeolites NaA and analcime using rice husk ash as silica source without using organic template,” *Journal of Materials Science*, vol. 45, pp. 5692–5697, 2010.
- [21] T. Fariás, L. C. de Ménorval, O. Picazo, and R. Jordán, “Ultrasonic and conventional synthesis of NaA zeolite from rice husk ash,” *Journal of Physics: Conference Series 792*, pp. 1–9, 2017.

- [22] A. R. Loiola, J. C. R. A. Andrade, J. M. Sasaki, and L. R. D. da Silva, "Structural analysis of zeolite NaA synthesized by a cost-effective hydrothermal method using kaolin and its use as water softener," *Journal of Colloid and Interface Science*, vol. 367, pp. 34–39, 2012.
- [23] E. Diaz, E. Munoz, A. Vega, and S. Ordonez, "Enhancement of the CO₂ retention capacity of X zeolites by Na- and Cs-treatments," *Chemosphere*, vol. 70, pp. 1375–1382, 2008.
- [24] R. Kodasma, J. Feroso, and A. Sanna, "Li-LSX-zeolite evaluation for post-combustion CO₂ capture," *Chemical Engineering Journal*, vol. 358, pp. 1351–1362, 2019.
- [25] P. Worathanakul and N. Rakpasert, "Different preparation methods of Ni-FAU(Y) zeolite for nitric oxide reduction," *International Journal of Chemical Engineering and Applications*, vol. 10, no. 4, pp. 106–109, 2019.
- [26] P. Worathanakul and P. Saisuwansiri, "Effect of copper and iron loading on zeolite Y for carbon dioxide adsorption," *The Journal of King Mongkut's University of Technology North Bangkok*, vol. 28, pp. 373–381, 2017.
- [27] S. J. Chen, M. Zhu, Y. Fu, Y. X. Huang, Z. C. Tao, and W. L. Li, "Using 13X, LiX, and LiPdAgX zeolites for CO₂ capture from post-combustion flue gas," *Applied Energy*, vol. 191, pp. 87–98, 2017.
- [28] E. Nyankson, J. K. Efavi, A. Yaya, G. Manu, K. Asare, J. Daafuor, and R. Y. Abrokwah, "Synthesis and characterisation of zeolite-A and Zn-exchanged zeolite-A based on natural aluminosilicates and their potential applications," *Cogent Engineering*, vol. 5, pp. 1–23, 2018.
- [29] D. Smykowski, B. Szyja, and J. Szczygieł, "DFT modeling of CO₂ adsorption on Cu, Zn, Ni, Pd/DOH zeolite," *Journal of Molecular Graphics and Modelling*, vol. 41, pp. 89–96, 2013.
- [30] D. Esquivel, A. J. Cruz-Cabeza, C. Jiménez-Sanchidrián, and F. J. Romero-Salguero, "Transition metal exchanged β zeolites: Characterization of the metal state and catalytic application in the methanol conversion to hydrocarbons," *Microporous and Mesoporous Materials*, vol. 179, pp. 30–39, 2013.
- [31] D. An, Y. Guo, Y. Zhu, and Z. Wang, "A green route to preparation of silica powders with rice husk ash and waste gas," *Chemical Engineering Journal*, vol. 162, pp. 509–514, 2010.
- [32] O. Cheung, Z. Bacsik, Q. Liu, A. Mace, and N. Hedin, "Adsorption kinetics for CO₂ on highly selective zeolites NaKA and nano-NaKA," *Applied Energy*, vol. 112, pp. 1326–1336, 2013.
- [33] P. Worathanakul, N. Klinpol, and T. Sarai, "Innovation of CO₂ adsorption with Li/zeolite A derived from bagasse ash," in *Proceeding of Universal Academic Cluster International Spring Conference in Osaka*, 2017, pp. 97–102.
- [34] C. A. Grande, H. Kvamsdal, G. Mondino, and R. Blom, "Development of moving bed temperature swing adsorption (MBTSA) process for post-combustion CO₂ capture: Initial benchmarking in a NGCC context," *Energy Procedia*, vol. 114, pp. 2203–2210, 2017.
- [35] K. A. Matori, M. M. Haslinawati, Z. A. Wahab, H. A. A. Sidek, T. K. Ban, and W. A. W. A. K. Ghani, "Producing amorphous white silica from rice husk," *MASAUM Journal of Basic and Applied Sciences*, vol. 1, pp. 512–515, 2009.
- [36] X. Jin, N. Jia, C. Song, D. Ma, G. Yan, and Q. Liu, "Synthesis of CHA zeolite using low cost coal fly ash," *Procedia Engineering*, vol. 121, pp. 961–966, 2015.
- [37] X. W. Cheng, Q. Y. Meng, J. Y. Chen, and Y. C. Long, "A facile route to synthesize mesoporous ZSM-5 zeolite incorporating high ZnO loading in mesopores," *Microporous and Mesoporous Materials*, vol. 153, pp. 198–203, 2012.
- [38] K. Ramasubramanian, M. A. Severance, P. K. Dutta, and W. S. W. Ho, "Fabrication of zeolite/polymer multilayer composite membranes for carbon dioxide capture: Deposition of zeolite particles on polymer supports," *Journal of Colloid and Interface Science*, vol. 452, pp. 203–214, 2015.
- [39] S. I. Garcés-Polo, J. Villarroel-Rocha, K. Sapag, S. A. Korili, and A. Gil, "Adsorption of CO₂ on mixed oxides derived from hydrotalcites at several temperatures and high pressures," *Chemical Engineering Journal*, vol. 332, pp. 24–32, 2018.
- [40] Y. Wang, T. Du, Z. Qiu, Y. Song, S. Che, and X. Fang, "CO₂ adsorption on polyethylenimine-modified ZSM-5 zeolite synthesized from rice husk ash," *Materials Chemistry and Physics*, vol. 207, pp. 105–113, 2018.
- [41] G. D. Pirngruber, V. Carlier, and D. Leinekugel-le-



Cocq, “Post-combustion CO₂ capture by vacuum swing adsorption using zeolites – A feasibility study,” *Oil & Gas Science and Technology*, vol. 69, pp. 989–1003, 2014.

[42] Y. Cho, J. Y. Lee, A. D. Bokare, S. B. Kwon, D. S.

Park, W. S. Jung, J. S. Choi, Y. M. Yang, J. Y. Lee, and W. Choi, “LiOH-embedded zeolite for carbon dioxide capture under ambient conditions,” *Journal of Industrial and Engineering Chemistry*, vol. 22, pp. 350–356, 2015.